

Sub-GeV Atmospheric Neutrinos and CP Violation in DUNE

Kevin J. Kelly,^{1,*} Pedro A. N. Machado,^{2,†} Ivan Martinez-Soler,^{2,3,4,‡}
 Stephen J. Parke,^{2,§} and Yuber F. Perez-Gonzalez^{2,3,4,||}

¹Theory Department, Fermi National Accelerator Laboratory, Batavia, Illinois 60510, USA

²Theory Department, Fermi National Accelerator Laboratory, P.O. Box 500, Batavia, Illinois 60510, USA

³Department of Physics & Astronomy, Northwestern University, Evanston, Illinois 60208, USA

⁴Colegio de Física Fundamental e Interdisciplinaria de las Américas (COFI), 254 Norzagaray street, San Juan, Puerto Rico 00901, USA

 (Received 22 April 2019; revised manuscript received 20 June 2019; published 23 August 2019)

We propose to use the unique event topology and reconstruction capabilities of liquid argon time projection chambers to study sub-GeV atmospheric neutrinos. The detection of low energy recoiled protons in DUNE allows for a determination of the leptonic CP -violating phase independent from the accelerator neutrino measurement. Our findings indicate that this analysis can exclude a range of values of δ_{CP} beyond the 3σ level. Moreover, the determination of the sub-GeV atmospheric neutrino flux will have important consequences in the detection of diffuse supernova neutrinos and in dark matter experiments.

DOI: [10.1103/PhysRevLett.123.081801](https://doi.org/10.1103/PhysRevLett.123.081801)

Introduction.—Atmospheric neutrinos, produced by cosmic-ray interactions in Earth’s atmosphere, have played a crucial role in the discovery of neutrino oscillations [1], the only evidence of nonzero neutrino masses [2,3]. Even now, atmospheric neutrinos contribute significantly to our understanding of neutrino oscillations and mixing in the lepton sector [4,5]. In this Letter, we are particularly interested in such neutrinos with energies in the 100 MeV to 1 GeV region, i.e., sub-GeV atmospheric neutrinos. The oscillation phenomenology of this sample is exceptionally rich [6–15]. The physical reason behind this is twofold. First, for baselines comparable to Earth’s radius, oscillation of sub-GeV neutrinos are strongly affected by both solar and atmospheric mass splittings. Second, the broad energy spectrum and large matter effects induced by Earth’s matter density profile lead to nontrivial oscillation effects, namely MSW [16,17] and parametric [18,19] resonances. Compared to long baseline accelerator neutrinos, the effects on oscillation probabilities of the leptonic CP -violating phase δ_{CP} is much more pronounced in sub-GeV atmospheric neutrinos, and, therefore, a measurement of their oscillation pattern can yield important new information on δ_{CP} .

At present, only Cherenkov light detectors like Super-Kamiokande and IceCube are large enough to have significant sensitivity to the broad spectrum of atmospheric

neutrinos. Nevertheless, a precise measurement of sub-GeV neutrinos is still lacking. The difficulty in studying these neutrinos is related to the event reconstruction, which is very challenging at these low energies. When a sub-GeV neutrino scatters on a nucleon via a charged current interaction, it produces a charged lepton and recoils the nucleon isospin partner, for instance $\nu_e n \rightarrow e^- p^+$. However, such low energy protons will not emit Cherenkov light in water, and thus are invisible in these detectors.

In neutrino scattering events, the kinematics of the outgoing lepton bears correlation with the neutrino energy and direction. Nevertheless, at these low energies, much of such correlation is lost, and there is a large spread in outgoing lepton momentum and angle. On top of that, the lack of charge identification impedes the separation of events originated from neutrinos or antineutrinos, concealing CP -violating effects. All this results in very poor reconstruction of the neutrino energy, direction, and flavor (between ν and $\bar{\nu}$), making the use of sub-GeV atmospheric neutrinos to probe CP violation in Cherenkov detectors impractical, unless detectors are gigantic, at the multi-megaton scale [20].

In liquid argon time projection chambers (LArTPCs), the situation is completely different. The LArTPC technology allows for excellent event topology reconstruction by detecting the tracks of all charged particles and identifying them by topology and energy loss. Recently it was shown that protons with kinetic energy above 21 MeV can be efficiently identified in the ArgoNeut experiment [21]. Their three momenta can still be reconstructed with good resolution, which will allow for a pioneering measurement of sub-GeV neutrino energies and angles. Besides, the

Published by the American Physical Society under the terms of the [Creative Commons Attribution 4.0 International license](https://creativecommons.org/licenses/by/4.0/). Further distribution of this work must maintain attribution to the author(s) and the published article’s title, journal citation, and DOI. Funded by SCOAP³.

capability of detecting these protons enables statistical separation between neutrinos and antineutrinos, since the former are significantly more likely to kick out a single proton from Argon than the latter [21]. Together with the fact that the cross section for neutrinos is about a factor of 2 larger than the one for antineutrinos, one expects that events with one lepton, one proton, and no pions (CC-1 $p0\pi$) are “neutrino rich,” while events with only an outgoing lepton (CC-0 $p0\pi$) are somewhat “antineutrino rich.”

In this Letter, we propose to use the unique event reconstruction capabilities of LArTPC to estimate how the future Deep Underground Neutrino Experiment (DUNE) [22] will be able to measure sub-GeV atmospheric neutrinos and extract information on δ_{CP} complementary to the accelerator neutrino program. We also comment on the impact of determining the sub-GeV atmospheric neutrino flux in diffuse supernova neutrino measurements and dark matter experiments.

Physics with low-energy atmospheric neutrinos.—In general terms, neutrino oscillations are driven by a phase α ($\Delta m_{ij}^2/eV^2$)(L/km)(GeV/E), where L is the distance traveled between neutrino production and detection, E is the neutrino energy, and $\Delta m_{ij}^2 \equiv m_i^2 - m_j^2$ is the squared mass splitting. When $E \gtrsim 1$ GeV, oscillations are induced largely by the aptly named atmospheric mass splitting $|\Delta m_{31}^2| \simeq 2.5 \times 10^{-3}$ eV² [23,24], and they develop over scales $L \sim \mathcal{O}(R_E)$, the radius of Earth. Oscillations of atmospheric neutrinos with energies $100 \text{ MeV} < E < 1$ GeV, are governed by both the atmospheric mass splitting and the smaller solar mass splitting, $\Delta m_{21}^2 \simeq 7.4 \times 10^{-5}$ eV² [25–30]. In what follows, we will consider two aspects of major significance to our analysis, CP violation and matter effects. We adopt the usual parametrization for neutrino mixing [31]. To set convention, we define the zenith angle such that $\cos \theta_z = -1$ corresponds to neutrinos coming from directly below the detector, while $\cos \theta_z = 0$ indicates the horizon direction.

First we discuss the effects of δ_{CP} in oscillations of sub-GeV neutrinos. In vacuum, for simplicity, the CP -violating term in neutrino oscillation probability is given by [32]

$$P_{CP} = -8J_r \sin \delta_{CP} \sin \Delta_{21} \sin \Delta_{31} \sin \Delta_{32}, \quad (1)$$

which includes the Jarlskog invariant [33,34] $J_r \sin \delta_{CP}$ (in our convention) and $\Delta_{ij} \equiv \Delta m_{ij}^2 L/4E$ are the oscillation phases. Oscillations of beam neutrinos probe the atmospheric splitting $\Delta_{31} \sim \mathcal{O}(1)$, while $\Delta_{21} \ll 1$. There, the CP term is suppressed by $\Delta m_{21}^2/\Delta m_{31}^2 \times \pi/2 \sim 1/20$ due to the fact that oscillations driven by Δm_{21}^2 do not have time to develop. This yields $P_{CP} \simeq -0.4J_r \sin \delta_{CP} \sin \Delta_{31} \sin \Delta_{32}$. Sub-GeV atmospheric neutrino oscillations, on the other hand, probe the solar splitting. In this case, the oscillations driven by $\Delta m_{31,32}^2$ are fast and average out. The resulting factor is just 1/2, leading to a much larger CP -violating term relative to beam neutrinos, namely $P_{CP} \simeq -4J_r \sin \delta_{CP} \sin \Delta_{21}$ with $\Delta_{21} \sim \mathcal{O}(1)$.

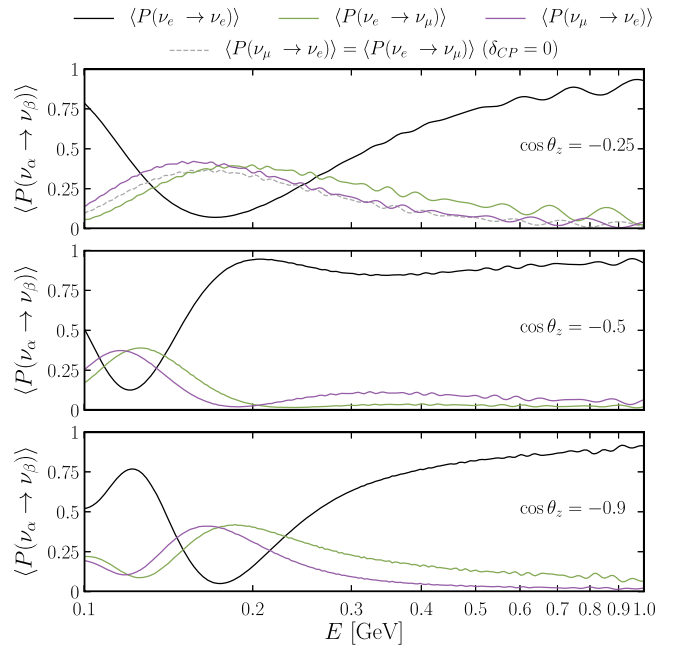


FIG. 1. Oscillation probabilities for $\nu_e \rightarrow \nu_e$ (black), $\nu_e \rightarrow \nu_\mu$ (green), and $\nu_\mu \rightarrow \nu_e$ (purple) for $\delta_{CP} = 3\pi/2$ and various values of the zenith angle $\cos \theta_z$ as indicated. In the upper panel we also present $P(\nu_\mu \rightarrow \nu_e) = P(\nu_e \rightarrow \nu_\mu)$ for $\delta_{CP} = 0$ in the upper panel (gray dashed). Earth’s matter profile was implemented using the PREM model [36].

In Fig. 1, we present three oscillation probability curves [35] as a function of neutrino energy for various zenith angles. A mild energy averaging of $10\%/\sqrt{E/\text{GeV}}$ was introduced which washes out unobservable fast oscillations induced by Δm_{31}^2 . In black, $P(\nu_e \rightarrow \nu_e)$ is displayed which does not depend on δ_{CP} . For $\delta_{CP} = 0$, the $\nu_e \rightarrow \nu_\mu$ and $\nu_\mu \rightarrow \nu_e$ transition probabilities are identical (upper panel, gray dashed line). The reason for that is because these oscillations are related by T parity and CPT is conserved. A nonzero δ_{CP} makes these probabilities distinct. In all panels we show $P(\nu_e \rightarrow \nu_\mu)$ and $P(\nu_\mu \rightarrow \nu_e)$ for $\delta_{CP} = 3\pi/2$ in green and purple, respectively. If these probabilities can be distinguished, then the CP phase can be measured. The second feature that stands out is the impact of different zenith angles, which is related to matter effects. We turn our attention to them now.

The second crucial feature of sub-GeV atmospheric neutrino oscillations are matter effects. Interactions with matter in the Earth, specifically in the dense mantle and core, may significantly modify neutrino oscillations. These effects are quite rich and have been studied in great depth [6–15]. Here we restrict ourselves to review some oscillation aspects and provide a few examples.

Up-going atmospheric neutrinos that traverse the Earth may go through an MSW resonance [16,17] in the solar sector, maximizing oscillations between ν_e and $\nu_{\mu,\tau}$, when

$$\Delta m_{21}^2 \cos \theta_{12} = 2\sqrt{2}EG_F n_e, \quad (2)$$

where G_F is the Fermi constant, and n_e is the electron number density. In the solar sector, the MSW resonance happens only for neutrinos, not for antineutrinos, as observed in oscillation of neutrinos produced in the Sun. We will focus on the $\nu_e \rightarrow \nu_e$ oscillation dependence on the zenith angle, shown as black curves in the different panels of Fig. 1. In the crust (upper panel, $-0.44 < \cos \theta_z$), mantle (middle panel, $-0.84 < \cos \theta_z < -0.44$), and core (bottom panel, $\cos \theta_z < -0.84$), the MSW resonant energies are found to be around 180, 130, and 50 MeV, respectively. Although this energy in Earth's core is below 100 MeV, another type of resonance occurs about $E \sim 170$ MeV, a parametric resonance [18,19,24]. A parametric resonance happens when changes to the matter density profile occur on the same scale as the neutrino oscillation length. The phenomenon is analogous to a resonant spring oscillator. Note that, due to the near-maximal value of θ_{23} , ν_e oscillates approximately equally into ν_μ and ν_τ .

The CP -violating and matter effects displayed in Fig. 1 show that the δ_{CP} effect is broad in neutrino energy, but there are large variations of oscillation curves for different zenith angles. Therefore, the precise reconstruction of the neutrino energy will not be as important as the determination of the incoming neutrino direction for the measurement of δ_{CP} . LArTPCs have excellent energy resolution and tracking reconstruction, and hence the incoming neutrino direction may be determined by considering the full event topology in charged current quasielastic events, $\nu_\ell n \rightarrow \ell^- p^+$.

Simulation details.—To simulate the atmospheric neutrino flux at sub-GeV energies, we use Ref. [37]. The atmospheric neutrinos flux for a given flavor is parametrized by

$$\Phi_\alpha(E) = \Phi_{\alpha,0} f_\alpha(E) \left(\frac{E}{E_0} \right)^\gamma, \quad (3)$$

where $f_\alpha(E)$ gives the shape of the neutrino energy spectrum for each flavor; $\Phi_{\alpha,0}$ is the normalization of flavor $\alpha = \nu_e, \nu_\mu, \bar{\nu}_e, \bar{\nu}_\mu$, E_0 is an arbitrary reference energy; and γ accounts for spectral distortions. To account for unknowns on the meson production in the atmosphere, we consider systematic uncertainties on the following quantities (see Supplemental Material [38] for details): overall normalization (40%); the ratio r_e between ν_e and ν_μ fluxes (5%); the ratio r_ν between neutrinos and antineutrinos fluxes (2%); and the spectral distortion parameter γ with 0.2 absolute uncertainty.

Neutrino events in DUNE will be classified by topology. We consider events with a charged lepton (electrons or muons) and up to two outgoing protons and no pions, namely $CC-Np0\pi$ ($N = 0, 1, 2$). Neutrino interactions were modeled with the NuWro event generator [39]. This is

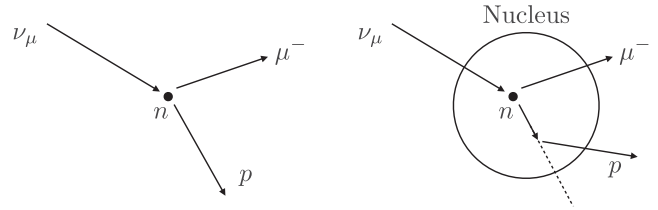


FIG. 2. Pictorial representations of a neutrino scattering on a free nucleon (left) and the effect of intranuclear cascades (right).

an important step as recoiled nucleons may reinteract still inside the nucleus, a process typically referred to as final state interactions or intranuclear cascades. A pictorial representation of neutrino scattering on free nucleons and the effect of intranuclear cascades is shown in Fig. 2. To account for detector response, a cut on the minimum proton kinetic energy of 30 MeV was implemented [22]. Momentum and angular resolutions of (5%,5%,10%) and (5°,5°,10°) for electrons, muons, and protons were assumed [40,41]. It has been shown that LArTPCs have a near 100% efficiency to reconstruct tracks [42], and thus we do not take efficiencies into account here.

We define two observables: the deposited energy E_{dep} (the sum of the energy of all detected particles) and deposited energy direction θ_z . For example, in a $CC-2p0\pi$ event we would have $E_{\text{dep}} = E_\ell + K_p^{(1)} + K_p^{(2)}$, where K_p indicates the proton kinetic energy. The direction is simply the direction of the sum all outgoing charged particles three momenta. Besides the imperfect detector response, intranuclear cascades effects and outgoing neutrons (which we consider to always go undetected) can affect distribution of E_{dep} and θ_z . We find that the largest contribution to the spread in deposited energy and direction arrives from intranuclear cascades [39]. A similar technique was proposed in Refs. [43,44] to improve the DUNE sensitivity for dark matter annihilation in the Sun using pointing.

To evaluate the experimental sensitivity to δ_{CP} , we have calculated the oscillation probabilities for $-1 \leq \cos \theta_z \leq 1$ and $100 \text{ MeV} \leq E_\nu \leq 1 \text{ GeV}$, assuming the PREM Earth density model [36] and marginalizing over other oscillation parameters assuming current central values and Gaussian priors on solar parameters [45] and expected priors from DUNE on atmospheric parameters [22], namely, $\sin^2 \theta_{12} = 0.31 \pm 0.013$, $\sin^2 \theta_{13} = 0.0224 \pm 0.00066$, $\sin^2 \theta_{23} = 0.58 \pm 0.01$, $\Delta m_{21}^2 = (7.39 \pm 0.21) \times 10^{-5} \text{ eV}^2$, and $\Delta m_{31}^2 = (+2.53 \pm 0.01) \times 10^{-3} \text{ eV}^2$. Throughout this Letter we assume an exposure of 400 kton-year. For the best fit values, we expect roughly 4000 ν_e , 5000 ν_μ , and 1000 $\bar{\nu}_e$ and $\bar{\nu}_\mu$ events. The majority of ν ($\bar{\nu}$) events are of the $CC-1p0\pi$ ($CC-0p0\pi$) topology. The backgrounds to this analysis are very small: beam events can be vetoed with timing information; cosmic ray backgrounds are expected to be suppressed by optical filtering techniques together with cuts on track length and topology [46]; and misidentified π^\pm

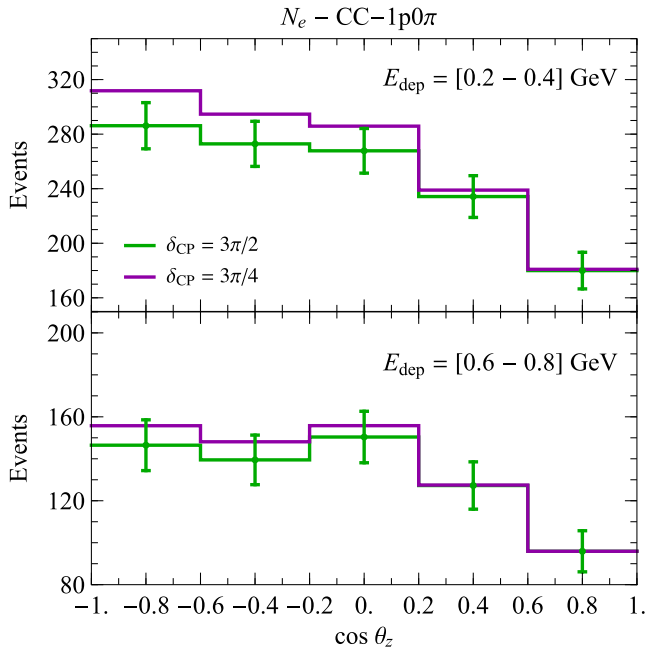


FIG. 3. Event spectra as a function of the zenith direction of the deposited energy θ_z , for $\delta_{CP} = 3\pi/2$ (green) and $\delta_{CP} = 3\pi/4$ (purple), and for a small subset of the entire data: deposited energies between 0.2–0.4 GeV (upper panel) and 0.6–0.8 GeV (lower panel). The error bars include only statistical uncertainties.

produced by higher energy neutrinos should be subleading, as they are suppressed by the lower fluxes, the neutral current cross section and the misidentification rate which should be below 10% [47].

In Fig. 3, $\cos\theta_z$ event spectra for a small subset of the data are shown for $\delta_{CP} = 3\pi/2$ (green) and $\delta_{CP} = 3\pi/4$ (purple). Two-dimensional event spectra in the $\cos\theta_z \times E_{\text{dep}}$ plane can be found in the Supplemental Material [38]. These spectra are used to calculate a χ^2 test statistics for each distinct final-state event topology, assuming no charge identification, but perfect $\mu - e$ separation. The sensitivity to δ_{CP} , presented in the following sections, comes from combining of all these event topologies and marginalizing the test statistics over the systematic uncertainties aforementioned.

Discussion.—The sensitivity to δ_{CP} for an input value of $\delta_{CP} = 3\pi/2$ is shown in Fig. 4. The individual $\Delta\chi^2$ contribution for each topology is shown, as well as the combined fit. A significant sensitivity to δ_{CP} may be achieved, allowing for excluding regions of the parameter space beyond the 3σ level.

Several factors contribute to this sensitivity. As already discussed, the CP violation effect for sub-GeV atmospheric neutrinos is a sizable effect, an order of magnitude larger than the corresponding one for beam neutrinos. To observe CP violation, one should be able to independently measure oscillations of neutrinos and antineutrinos and/or the time-conjugated channels $\nu_\mu \rightarrow \nu_e$ and $\nu_e \rightarrow \nu_\mu$. At these low energies, a neutrino interaction is more likely to kick out a

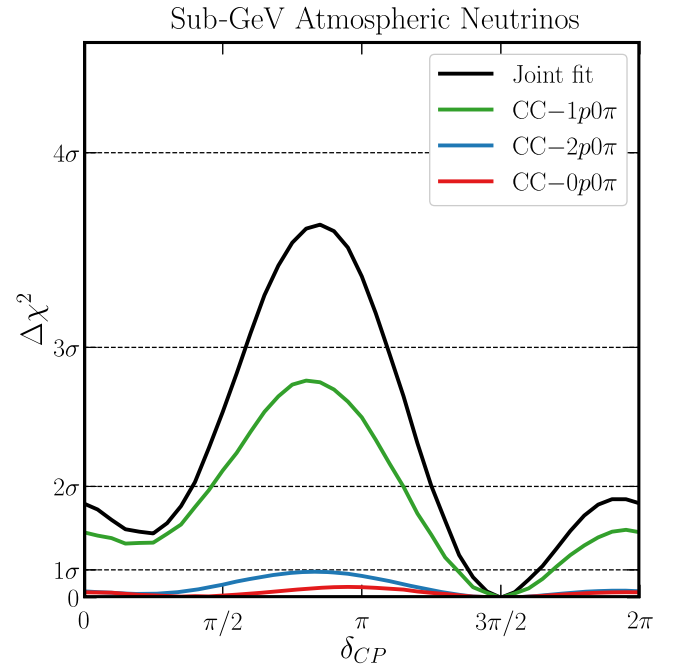


FIG. 4. DUNE sensitivity to the leptonic CP -violating phase δ_{CP} using sub-GeV atmospheric neutrinos, for an input value $\delta_{CP} = 3\pi/2$ and 400 kton-year exposure.

proton from a nucleus than an antineutrino interaction, and vice-versa for neutrons—therefore, the $CC-1p0\pi$ sample is neutrino rich while $CC-0p0\pi$ is antineutrino rich. Combining these two samples allows for measuring, statistically, the flux of ν and $\bar{\nu}$ from the atmosphere. Besides, θ_z has a typical spread between $\Delta\theta \sim 20^\circ-30^\circ$, mainly due to intranuclear cascades, except for the $CC-0p0\pi$ topology which has $\Delta\theta \sim 50^\circ$. This allows us to disentangle the baseline dependent oscillation effects discussed earlier fairly well. These aspects indicate a synergy between each distinct topology, as it can be seen in Fig. 4: the sum of the individual $\Delta\chi^2$ contributions for each topology is significantly below the combined sensitivity.

We have found that DUNE constrains the pull parameters beyond the uncertainties adopted here, namely (2%, 2%, 1%, 0.02) for $(\Phi_0, r_e, r_\nu, \gamma)$, evidencing that the experimental sensitivity is not induced by any prior uncertainty on the atmospheric fluxes, and therefore is quite robust (see Supplemental Material [38] for details). As we see in Fig. 3, the effects of δ_{CP} on the atmospheric spectra are highly nontrivial. Therefore, the available range energies and baselines (given by θ_z) helps to disentangle these effects from the several uncertainties in the sub-GeV atmospheric neutrino flux. This will have significant consequences for determining the atmospheric background in diffuse supernovae neutrino measurements [48] and dark matter experiments [49].

The sensitivity to δ_{CP} obtained here, though not as powerful as the one obtained with beam neutrinos [50], is competitive, providing an important cross check for the

determination of δ_{CP} involving different energies and baselines. The sensitivity to δ_{CP} is mostly encoded by neutrinos with energies below ~ 0.6 GeV, while it is mainly limited by statistics and the spread in θ_z distribution. The addition of multi-GeV atmospheric neutrinos and other event topologies, should improve the sensitivity to δ_{CP} and new physics scenarios [51]. Furthermore, other oscillation parameters can be constrained with this analysis. As an example we show the sensitivity in $\delta_{CP} \times \sin^2 \theta_{23}$ in the Supplemental Material [38]. A similar analysis could be performed for the JUNO experiment [52].

Finally, one could wonder about the impact of neutrino interaction uncertainties in this analysis. Overall cross section uncertainty plays no role as it is degenerate with the flux normalization. Intranuclear cascade uncertainties are expected to be more relevant and we will investigate this in detail in a forthcoming publication. The exploration of these effects is quickly evolving with the liquid argon neutrino program [21], and we expect significant advances by the time DUNE will be taking data. In fact, the short-baseline neutrino program [53] at Fermilab and DUNE itself will explore the sub-GeV region with high statistics using beam neutrinos. The DUNE-PRISM concept [54], a movable near detector to probe off-axis neutrinos, could greatly enhance our knowledge of neutrino-argon interactions at sub-GeV energies if the near detector hall allows for an off-axis distance of at least 25–30 meters. This would enable a pioneering data-driven analysis of CP violation using sub-GeV atmospheric neutrinos in DUNE, fully exploring the unique capabilities of liquid argon time projection chambers.

Conclusions.—We have proposed to use the unique capabilities of LArTPCs to explore the physics of sub-GeV atmospheric neutrinos. By detecting low energy charged particles, the direction and energy of incoming neutrinos can be inferred, furnishing LArTPCs with a unique opportunity to probe CP violation with sub-GeV atmospheric neutrinos. We have shown, with a detailed simulation, that DUNE’s sensitivity to the CP phase from this atmospheric sample is competitive, possibly ruling out regions of the parameter space beyond the 3σ level, and providing an important cross-check of the CP phase determination with beam neutrinos. This measurement will have significant consequences for diffuse supernovae neutrino measurements and dark matter experiments. We also highlight the possibility of performing a data-driven analysis using inputs from highly off-axis DUNE-PRISM measurements on neutrino-argon interactions.

We thank Alvaro Hernandez-Cabezudo, Shirley Li, Bryce Littlejohn, Alberto Marchionni, Ornella Palamara, and Sam Zeller for useful discussions. We are especially grateful to John Beacom for his comments on an earlier version of this manuscript which led to substantial improvement. Fermilab is operated by the Fermi Research Alliance, LLC under contract No. DE-AC02-07CH11359

with the United States Department of Energy. This project has received funding/support from the European Unions Horizon 2020 research and innovation program under the Marie Skłodowska-Curie Grant Agreement No. 690575 and No. 674896. I. M. S. and Y. P. G. acknowledge travel support from the Colegio de Fisica Fundamental e Interdisciplinaria de las Americas (COFI).

*kkelly12@fnal.gov

†pmachado@fnal.gov

‡ivan.martinezsoler@northwestern.edu

§parke@fnal.gov

||yfperezg@northwestern.edu

- [1] Y. Fukuda *et al.* (Super-Kamiokande Collaboration), *Phys. Rev. Lett.* **81**, 1562 (1998).
- [2] T. Kajita, *Rev. Mod. Phys.* **88**, 030501 (2016).
- [3] A. B. McDonald, *Rev. Mod. Phys.* **88**, 030502 (2016).
- [4] K. Abe *et al.* (Super-Kamiokande Collaboration), *Phys. Rev. D* **97**, 072001 (2018).
- [5] M. G. Aartsen *et al.* (IceCube Collaboration), *Phys. Rev. Lett.* **120**, 071801 (2018).
- [6] V. D. Barger, T. J. Weiler, and K. Whisnant, *Phys. Lett. B* **440**, 1 (1998).
- [7] A. Friedland, C. Lunardini, and M. Maltoni, *Phys. Rev. D* **70**, 111301(R) (2004).
- [8] P. Huber, M. Maltoni, and T. Schwetz, *Phys. Rev. D* **71**, 053006 (2005).
- [9] E. K. Akhmedov, M. Maltoni, and A. Yu. Smirnov, *J. High Energy Phys.* **06** (2008) 072.
- [10] O. Mena, I. Mocioiu, and S. Razzaque, *Phys. Rev. D* **78**, 093003 (2008).
- [11] O. L. G. Peres and A. Yu. Smirnov, *Phys. Rev. D* **79**, 113002 (2009).
- [12] E. Fernandez-Martinez, G. Giordano, O. Mena, and I. Mocioiu, *Phys. Rev. D* **82**, 093011 (2010).
- [13] V. Barger, R. Gandhi, P. Ghoshal, S. Goswami, D. Marfatia, S. Prakash, S. K. Raut, and S. U. Sankar, *Phys. Rev. Lett.* **109**, 091801 (2012).
- [14] E. K. Akhmedov, S. Razzaque, and A. Yu. Smirnov, *J. High Energy Phys.* **02** (2013) 082; **07** (2013) 26.
- [15] W. Winter, *Phys. Rev. D* **88**, 013013 (2013).
- [16] L. Wolfenstein, *Phys. Rev. D* **17**, 2369 (1978).
- [17] S. P. Mikheyev and A. Yu. Smirnov, *Sov. J. Nucl. Phys.* **42**, 913 (1985).
- [18] E. K. Akhmedov, *Yad. Fiz.* **47**, 475 (1988) [*Sov. J. Nucl. Phys.* **47**, 301 (1988)].
- [19] P. I. Krastev and A. Yu. Smirnov, *Phys. Lett. B* **226**, 341 (1989).
- [20] S. Razzaque and A. Yu. Smirnov, *J. High Energy Phys.* **05** (2015) 139.
- [21] O. Palamara (ArgoNeuT Collaboration), *J. Phys. Soc. Jpn. Conf. Proc.* **12**, 010017 (2016).
- [22] R. Acciarri *et al.* (DUNE Collaboration), [arXiv:1512.06148](https://arxiv.org/abs/1512.06148).
- [23] M. A. Acero *et al.* (NOvA Collaboration), *Phys. Rev. D* **98**, 032012 (2018).
- [24] K. Abe *et al.* (T2K Collaboration), *Phys. Rev. Lett.* **121**, 171802 (2018).

- [25] A. Gando *et al.* (KamLAND Collaboration), *Phys. Rev. D* **88**, 033001 (2013).
- [26] B. T. Cleveland, T. Daily, R. Davis, Jr., J. R. Distel, K. Lande, C. K. Lee, P. S. Wildenhain, and J. Ullman, *Astrophys. J.* **496**, 505 (1998).
- [27] J. N. Abdurashitov *et al.* (SAGE Collaboration), *Phys. Rev. C* **80**, 015807 (2009).
- [28] G. Bellini *et al.*, *Phys. Rev. Lett.* **107**, 141302 (2011).
- [29] J. Hosaka *et al.* (Super-Kamiokande Collaboration), *Phys. Rev. D* **73**, 112001 (2006).
- [30] B. Aharmim *et al.* (SNO Collaboration), *Phys. Rev. C* **88**, 025501 (2013).
- [31] M. Tanabashi *et al.* (Particle Data Group), *Phys. Rev. D* **98**, 030001 (2018).
- [32] P. B. Denton, H. Minakata, and S. J. Parke, *J. High Energy Phys.* **06** (2016) 051.
- [33] C. Jarlskog, *Phys. Rev. Lett.* **55**, 1039 (1985).
- [34] C. Jarlskog, *Z. Phys. C* **29**, 491 (1985).
- [35] See <https://imgur.com/HoWUniu> for an animation of how δ_{CP} changes oscillation probabilities as a function of zenith angle and neutrino energy.
- [36] A. M. Dziewonski and D. L. Anderson, *Phys. Earth Planet. Interiors* **25**, 297 (1981).
- [37] M. Honda, M. Sajjad Athar, T. Kajita, K. Kasahara, and S. Midorikawa, *Phys. Rev. D* **92**, 023004 (2015).
- [38] See Supplemental Material at <http://link.aps.org/supplemental/10.1103/PhysRevLett.123.081801> for further discussions on the relevant oscillation probabilities, differential event rates per event topology, as well as further considerations regarding systematic uncertainties and the statistical treatment of the current determination of oscillation parameters.
- [39] T. Golan, J. T. Sobczyk, and J. Zmuda, *Nucl. Phys. B, Proc. Suppl.* **229–232**, 499 (2012).
- [40] R. Acciarri *et al.* (ArgoNeuT Collaboration), *Phys. Rev. D* **90**, 012008 (2014).
- [41] T. Alion *et al.* (DUNE Collaboration), [arXiv:1606.09550](https://arxiv.org/abs/1606.09550).
- [42] R. Acciarri *et al.* (MicroBooNE Collaboration), *J. Instrum.* **12**, P12030 (2017).
- [43] C. Rott, S. In, J. Kumar, and D. Yaylali, *J. Cosmol. Astropart. Phys.* **01** (2017) 016.
- [44] C. Rott, D. Jeong, J. Kumar, and D. Yaylali, *J. Cosmol. Astropart. Phys.* **07** (2019) 006.
- [45] I. Esteban, M. C. Gonzalez-Garcia, A. Hernandez-Cabezudo, M. Maltoni, and T. Schwetz, *J. High Energy Phys.* **01** (2019) 106.
- [46] C. Adams *et al.* (MicroBooNE Collaboration), [arXiv:1812.05679](https://arxiv.org/abs/1812.05679).
- [47] J. N. Esquivel, μ/π separation using convolutional neural networks for the MicroBooNE charged current inclusive cross section measurement, Ph.D. thesis, Syracuse University, 2018.
- [48] J. F. Beacom, *Annu. Rev. Nucl. Part. Sci.* **60**, 439 (2010).
- [49] A. Gütlein, C. Ciemniak, F. von Feilitzsch, N. Haag, M. Hofmann, C. Isaila, T. Lachenmaier, J.-C. Lanfranchi, L. Oberauer, S. Pfister, W. Potzel, S. Roth, M. von Sivers, R. Strauss, and A. Zöller, *Astropart. Phys.* **34**, 90 (2010).
- [50] B. Abi *et al.* (DUNE Collaboration), [arXiv:1807.10334](https://arxiv.org/abs/1807.10334).
- [51] K. J. Kelly, P. A. N. Machado, I. Martinez-Soler, S. J. Parke, and Y. F. Perez-Gonzalez (to be published).
- [52] F. An *et al.* (JUNO Collaboration), *J. Phys. G* **43**, 030401 (2016).
- [53] P. A. Machado, O. Palamara, and D. W. Schmitz, *Annu. Rev. Nucl. Part. Sci.* **69** (2019).
- [54] T. Cai, J. Calcutt, K. Mahn, L. Pickering, S. Manly, H. Tanaka, C. Vilela, M. Wilking, and G. Yang, The dune-prism near detector, 2018, <https://indico.fnal.gov/event/16205/contribution/2/material/0/0.pdf>.